OH-Initiated Oxidation of Toluene. 3. Low-Energy Routes to Cresol and Oxoheptadienal

Terry J. Frankcombe†

Physical Chemistry, Department of Chemistry, Göteborg University, SE-412 96 Göteborg, Sweden

Received: October 29, 2007; In Final Form: December 12, 2007

The toluene−OH−O_2 system implicated in the atmospheric degradation of toluene is studied further using quantum chemistry methods. Two new reaction mechanisms are explored as alternatives to the previously proposed mechanism. While the previous mechanism involves surmounting a 170 kJ/mol barrier, the new equivalent cresol formation route has a barrier above the asymptotic state calculated to be 12 kJ/mol at the B3LYP/6-311G(2df,2pd) level. The new oxoheptadienal formation route occurs via two successive reactions with OH, with the highest barrier lying 200 kJ/mol below the energy of the reactants. Neither of the newly proposed reaction mechanisms involves forming a toluene oxide intermediate.

1. Introduction

Reactions involving toluene are of great interest in atmospheric chemistry, with toluene being the most abundant aromatic species in Earth's atmosphere and playing a central role in urban ozone and organic aerosol production. Atmospheric aromatic degradation processes are not understood in detail but are known to be dominated by reactions with hydroxyl radicals. The aromatic−OH adducts then go on to react with molecular oxygen.[1]

This is the third in a series of papers exploring possible toluene degradation reactions. The first paper[2] (hereafter referred to as paper 1) describes extensive quantum chemistry calculations of a possible reaction path in which the initial toluene−OH adduct is attacked by oxygen to remove the hydroxy hydrogen atom as HO_2, followed by isomerization and subsequent OH-addition and O_2-mediated hydrogen abstraction steps, yielding toluene oxides, cresols, and oxoheptenal. This investigation was based on the mechanism proposed by Klotz et al.[3] In the second paper[4] (referred to as paper 2), a subset of the species identified in paper 1 are used in a master equation description to model the toluene oxide photolysis experiments of Klotz et al. The results of that modeling reproduce some key trends in the experimental findings, though the time scales are significantly different.

An unusual feature of the reaction path determined in paper 1 and modeled in paper 2 is the calculated minimum energy paths (MEPs) from toluene oxides to cresols. These isomerizations proceed in two distinct steps in which the involved hydrogen atom migrates to an adjacent carbon atom, allowing the bridging oxygen atom to form a ketone intermediate, before the hydrogen migrates back to form the cresol. The more obvious paths (such as forming the hydroxy fragment first, or "insertion" into the C−H bond) do not occur along the MEPs. The potential energy along these MEPs presents substantial barriers to the isomerization reaction, of the order 150−200 kJ/mol. Clearly, any alternate path with a substantially lower barrier would compete effectively with this hydrogen-shuffling mechanism.

In this work we move away from the mechanism proposed by Klotz et al., primarily to avoid the high barriers associated with reactions to form and then isomerize toluene oxide. It shall be shown that the cresol and 6-oxo-2,4-heptadienal products of the mechanism proposed by Klotz et al. can be reached by reaction paths that avoid forming toluene oxide.

2. Method

The computational methodology was very similar to that used in paper 1. The Gaussian 03 package[5] was used for all calculations. Calculations were performed at the B3LYP/6-311G(2df,2pd) level of theory, previously shown to yield good results for this system.[2]

For all species and configurations considered the geometry was relaxed to give the minimum energy configuration. For all the reaction paths considered, saddle points on the minimum energy paths were located by initially performing partial relaxations with likely reaction-coordinate-like bond lengths fixed and scanned. The highest energy partially relaxed geometry was used as the starting guess for an STQN saddle point search.[6,7] Harmonic vibrational analysis was performed at all stationary points. All energies reported here include zero-point energy (ZPE) contributions, with the ZPE being scaled by 0.9670 from the pure harmonic value. All energies are plotted relative to the energy of the initial toluene system (with appropriate free O_2 and OH radical energies added).

The species labeling scheme used in this paper is a continuation of that used in papers 1 and 2. Thus, newly characterized species begin with number **38**.

3. Results

The reaction paths calculated in this work are summarized in Figure 1, which also shows some of the energies along the mechanism of Klotz et al. calculated previously and reported in paper 1. Only paths from the *ortho*-toluene−OH adduct are shown. The structures of the various species are shown in Figures 2−4. Note that the isomers of hydroxymethylcyclohexadienyl (**2**) (themselves radical isomers of cresols) were incorrectly labeled as hydroxycyclohexadienyls in papers 1 and 2.

3.1. Low-Energy Route to Cresol. In the paths identified in paper 1, the addition of OH to toluene is followed by removal of the hydroxide hydrogen atom. This abstraction occurs in a number of steps starting with the formation of a toluene−OH

† E-mail: terry@chem.gu.se; T.Frankcombe@chem.leidenuniv.nl.

10.1021/jp710446r CCC: $40.75
Published on Web 01/29/2008

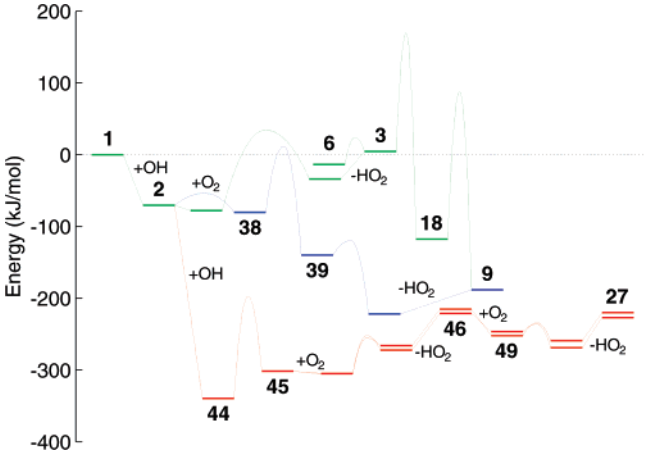

Figure 1. Calculated MEPs of routes from the toluene−OH adduct *ortho*-**2** to *o*-cresol **9** and to 6-oxo-2,4-heptadienal (**27**). ZPE-corrected energies are shown relative to separated toluene, OH, and O_2 fragments. Energies from paper 1 following the mechanism proposed by Klotz et al. are shown in green, those from the alternate hydrogen abstraction route (section 3.1) are shown in blue, and those for the formation of **27** after addition of a second OH (section 3.2) are shown in red.

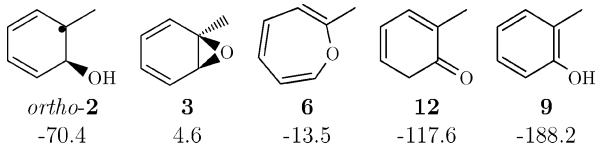

ortho-**2** -70.4 | **3** 4.6 | **6** -13.5 | **12** -117.6 | **9** -188.2

Figure 2. Species from paper 1 involved in the formation of cresol **9** from the *ortho*-toluene−OH adduct **2**, via toluene oxide **3**, and the relative ZPE-orrected ground-state energy (kJ/mol).

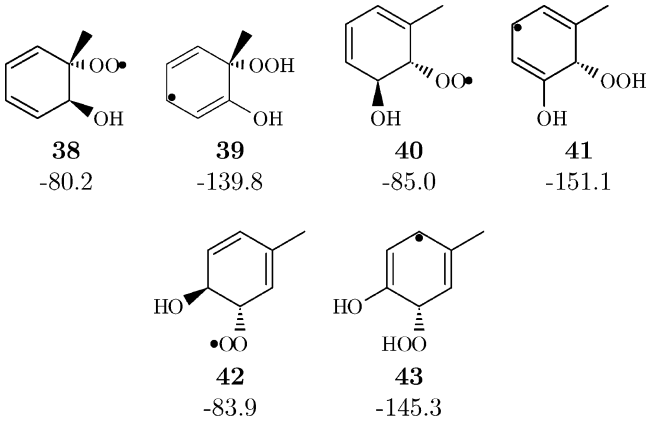

38 -80.2 | **39** -139.8 | **40** -85.0 | **41** -151.1

42 -83.9 | **43** -145.3

Figure 3. Species involved in the formation of *o*-, *m*-, and *p*-cresol following O_2 addition to toluene−OH adducts and the relative ZPE-corrected ground-state energy (kJ/mol).

adduct···oxygen molecule complex. The hydrogen atom migration from the toluene derivative to the oxygen molecule is associated with the simultaneous formation of the epoxide structure of toluene oxide. As indicated in Figure 1, a much lower energy process is the endwise reactive addition of the oxygen molecule to the ring of the toluene−OH adduct. Not only was the barrier to this addition much lower than that for the previously identified toluene oxide formation path (with a MEP lying well below the energy of the separated toluene, hydroxyl, and oxygen fragments), but the peroxyl radicals so formed were found to be more stable than the prereactive complex by 10−15 kJ/mol.

Clearly, there are multiple sites to which the oxygen atom can bind, even from a particular hydrogen bound complex. A number of studies[8−11] have shown that addition of oxygen

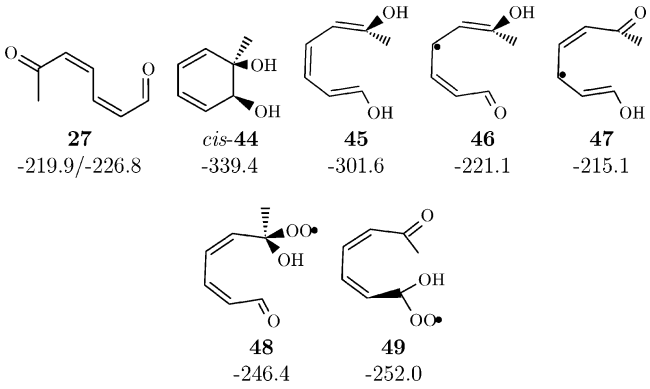

27 -219.9/-226.8 | *cis*-**44** -339.4 | **45** -301.6 | **46** -221.1 | **47** -215.1

48 -246.4 | **49** -252.0

Figure 4. Species involved in the formation of 6-oxo-2,4-heptadienal (**27**) by the addition of a second OH radical to the *ortho*-toluene−OH adduct and the relative ZPE-corrected ground state energy (kJ/mol).

molecules to *ortho*-**2** is energetically most favorable at carbon 3, cis to the hydroxide group bonded to the ring. The second most favorable position is again cis, at carbon 1, the formal radical site indicated in Figure 2. However, these reactions leave the peroxyl fragment inaccessible to the hydrogen atom bonded to the same carbon as the hydroxy group. In this work only those products relevant to the subsequent formation of cresol shall be reported. Thus, we are interested in the products of adding the oxygen molecule to the other side of the ring, trans to the hydroxide. These products are slightly higher in energy than the corresponding cis adduct. Also, within the possible adducts with the added O_2 fragment trans to the OH group, the energetics alone did not determine the choice made for reporting here. For example, addition of O_2 to carbon 6 of *ortho*-**2** resulted in a structure 6 kJ/mol more stable than the addition to carbon 2 that produces **38**. However, like for the trans adducts, the subsequent reaction steps leading to the cresols were not accessible from this adduct.

The hydrogen atom bonded to the same carbon atom as the hydroxyl group in **38** could be migrated to the added peroxyl group to form a hydroperoxide **39**. This rearrangement involves a substantial reorganization of the bonding with the molecule and occurs over a barrier extending above the asymptotic fragment energies by 12 kJ/mol (slightly lower along the paths from *meta*- and *para*-**2**). This turned out to be the critical step in the formation of cresol by the path identified in this work. Not only was this the highest barrier on the path, avoiding the breakup of the hydroxyl fragment meant toluene oxide need not be formed. Thus the high energy and complicated hydrogen migration paths identified in paper 1 need not be traversed.

From the hydroperoxy-cresol **39** the HO_2 group could readily be dissociated over a small barrier to form a van der Waals complex. The most stable structure identified along this reaction path was this complex of *o*-cresol hydrogen bonded to HO_2. The substantial reduction in energy coming from reestablishing full aromaticity in the carbon ring contributes to the large stabilization of the cluster relative to the hydroperoxide. A substantial stabilization also came from the hydrogen bonding between the fragments in the van der Waals cluster, as this structure was found to be more than 30 kJ/mol more stable than the separated fragments. However, the fact that the energy of the complex lies more than 220 kJ/mol below the entrance channel means that the cluster would dissociate, with a substantial fraction of the excess energy being converted to relative kinetic energy of the cresol and HO_2 fragments.

Similar paths to those described for the *ortho*-toluene−OH adduct were found for O_2 addition to the *meta* and *para* adducts. These paths are not shown in Figure 1. While the *meta*-toluene−

OH adduct lay slightly higher in energy than the ortho adduct, the intermediates **40** and **41** were found to be lower in energy than the equivalent structures on the *ortho* path by 5 and 11 kJ/mol, respectively. Additionally, the barrier for the formation of **40** from the complex of molecular oxygen with *meta*-**2** occurred over a much lower barrier than for the *ortho* path. On the other hand, the barrier to hydrogen migration from the carbon ring to the end of the peroxyl radical group (the highest barrier along this path) was very similar for both the *ortho* and *meta* paths. The energies along the analogous path for the *para*-toluene−OH adduct were generally intermediate between those for the *ortho* and *meta* paths. No analogous path is possible for the *ipso*-toluene−OH adduct.

3.2. Low-Energy Route to 6-Oxo-2,4-heptadienal. Clearly, the toluene−OH adduct **2** forms in an environment containing free OH radicals. Thus an encounter with a second OH radical is possible. The radical−radical reaction between *ortho*-**2** and OH resulted in a very stable diol **44**, lying around 270 kJ/mol below the energy of the *ortho*-**2** + OH state. The second OH fragment could be added in either a cis or trans configuration to the existing hydroxide group. The cis form lay 10 kJ/mol lower in energy than the trans form and was the form considered for subsequent steps in this work.

Forming **27** from **44** required the stripping off of the hydrogen atoms from the two hydroxyl groups and a ring opening. Removal of the hydrogen atoms before the ring was broken would result in a ketone with hypervalent carbon atoms in the ring, a high-energy diradical or a cyclic peroxide, formed via a concerted H_2 elimination. No such paths were found.

From *cis*-**44**, the carbon ring could break between the substituent hydroxide groups by passing over a 142 kJ/mol barrier. The top of this barrier lay almost 200 kJ/mol below the initial toluene + 2OH energy (almost 130 kJ/mol below the initial toluene−OH adduct), so more than enough energy would be available in the system to cross this barrier. While breaking other bonds has not been investigated in this work, examining the carbon−carbon bond lengths suggests that this bond is likely to be the weakest of the ring, being 3% longer than the next longest bond at the potential minimum configuration. The resulting hept-1,3,5-trien-1,6-diol (**45**) lay 38 kJ/mol above *cis*-**44**.

The hydrogen atoms of the hydroxyl groups could be attacked by oxygen molecules before elimination as HO_2, as on the other paths investigated in paper 1. Two subsequent reaction paths (and hence two complexes) were considered in this work, corresponding to removing one or the other of the two hydroxide hydrogen atoms first. Van der Waals complexes of **45** with O_2 were found to be bound by less than 4 kJ/mol. Migration of the hydrogen atoms to form complexes containing HO_2 fragments was found to occur over barriers around 50 kJ/mol high, resulting in **46** and **47** once the product complexes dissociated. The second hydroxyl hydrogen atom could be removed in each case by reaction with molecular oxygen again but only following reactive addition of the O_2 to the carbon backbone. These paths, via **48** and **49**, were similar to the first step in the low-energy route to cresol described above. (Only **46** and **49** are labeled in Figure 1 due to space constraints.) However, in these cases initial van der Waals minima with the O_2 hydrogen bonded to the relevant hydroxyl group (not shown in Figure 1) facilitated the reactive addition without the presence of an energy barrier above the energy of the parent species **46** and **47**. No path could be found to migrate the hydrogen atoms to the oxygen molecules bound in these van der Waals complexes without first attaching the O_2 in the form of **48** and **49**.

In these final steps before the formation of the product **27**, HO_2 fragments were formed by migration of the hydrogen atom to the peroxyl fragment with simultaneous breaking of the peroxyl oxygen−carbon bond. The energy cost of this migration and simultaneous bond breaking was offset by the energy gained in reestablishing the hydrogen bonding between the HO_2 fragments and the nascent ketone oxygen. This binding energy was around 40 kJ/mol. The hydrogen migration and fragmentation barrier from **49** (**48**) was less than 18 kJ/mol (10 kJ/mol).

The two routes from the diol **45** to the product **27** (abstraction from the primary or secondary alcohol first) produced two different isomers of **27** when following along the MEPs. These were related by a simple rotation around the single bond between carbons 5 and 6, swapping the orientation of the ketone and methyl fragments. The isomers were separated in energy by 7 kJ/mol and could readily interconvert via a transition state 5 kJ/mol above the energy of the higher isomer. Along the two MEPs from **45**, the rotation of the relevant groups occurred as the oxygen molecule attached to the carbon backbone to form **48** from **46** (as opposed to the path from **47** to **49**, where no such rotation occurred).

4. Discussion and Conclusion

As indicated in Figure 1, the new paths investigated in this work present significantly lower energy barriers than the paths followed in papers 1 and 2. The reaction path described in section 3.1,

$$\text{toluene} + \text{OH} + \text{O}_2 \rightarrow \text{cresol} + \text{HO}_2 \qquad (1)$$

along the MEP involves crossing a maximum barrier 12 kJ/mol above the initial toluene state. The previously determined path, also described overall by (1), involves overcoming a barrier of 170 kJ/mol. On energetics alone one would expect that under thermal conditions reactions along the path determined in this work would occur many orders of magnitude faster than along the previously characterized path.

The main difference between the two cresol formation mechanisms—aside from the obvious initial step of reactive association of the O_2 fragment in the new path versus reaction from the oxygen-containing van der Waals complex in the previously characterized path—is the identity of the hydrogen atom removed as HO_2. The mechanism proposed by Klotz et al. strips the hydrogen atom from the hydroxide group added in the initial step, forming toluene oxide. The hydroxide group must be reformed to produce cresol, requiring that the extracted hydrogen be replaced by hydrogen migration. The path proposed in this work, however, leaves the hydroxide group intact and removes the excess hydrogen atom directly.

The second path described in this work (section 3.2) can be described similarly as

$$\text{toluene} + 2\text{OH} + 2\text{O}_2 \rightarrow \text{oxoheptadienal} + 2\text{HO}_2 \qquad (2)$$

This path is even more energetically favorable. The highest barrier on this path lies almost 200 kJ/mol below the energy of the initial toluene + OH + O_2 state. The exothermic reaction of the initial toluene−OH adduct with the second OH radical liberates more than enough energy into the internal modes of the product **44** to overcome the barriers along the subsequent reaction path without the need for further excitation. Thus, the speed of reaction on this path depends not so much on energetics as on the steric factors involved in the collisions of the reactants.

Many potential side reactions have been ignored in this work. Such side reactions include the addition of O_2 to **2** at other

carbon sites or on the other side of the ring, as discussed in section 3.1, and reaction from *trans*-**44**.

The energies reported in paper 1 were said to be "broadly consistent with the mechanism proposed by Klotz et al." However it was obvious that the calculated barriers would present serious obstacles to thermal reaction. The paths investigated in this work do not suffer from such clear drawbacks. Thus, one must conclude that the present paths are more plausible than those of Klotz et al. While reaction with an aromatic oxide intermediate step appears to be well supported for benzene photooxidation,[3] an analogous mechanism for toluene is unlikely. The paths explored in this work, described overall by (1) and (2), also produce the high HO_2 yields from reaction with O_2 for which the mechanism of Klotz et al. was notable.

It is worth noting that the experiments of Klotz et al.[3] were not designed to directly study the photooxidation of toluene but rather a part of their proposed mechanism assuming toluene oxide as an intermediate. Thus, the existence of significantly lower energy paths for the OH-initiated oxidation of toluene does not cast doubt on the results published in paper 2 of this series. The modeling performed in that work is directly analogous to the toluene oxide photolysis studied by Klotz et al.

Supporting Information Available: Geometries, energies, and frequencies of the stationary points described in this work compiled into a PDF document. This material is available free of charge via the Internet at http://pubs.acs.org.

References and Notes

(1) Atkinson, R. *Atmos. Environ*. **2000**, *34*, 2063.
(2) Frankcombe, T. J.; Smith, S. C. *J. Phys. Chem. A* **2007**, *111*, 3686.
(3) Klotz, B.; Barnes, I.; Golding, B. T.; Becker, K.-H. *Phys. Chem. Chem. Phys*. **2000**, *2*, 227.
(4) Frankcombe, T. J.; Smith, S. C. *J. Phys. Chem. A* **2007**, *111*, 3691.
(5) Frisch, M. J.; Trucks, G. W.; Schlegel, H. B.; Scuseria, G. E.; Robb, M. A.; Cheeseman, J. R.; Montgomery, J. A., Jr.; Vreven, T.; Kudin, K. N.; Burant, J. C.; Millam, J. M.; Iyengar, S. S.; Tomasi, J.; Barone, V.; Mennucci, B.; Cossi, M.; Scalmani, G.; Rega, N.; Petersson, G. A.; Nakatsuji, H.; Hada, M.; Ehara, M.; Toyota, K.; Fukuda, R.; Hasegawa, J.; Ishida, M.; Nakajima, T.; Honda, Y.; Kitao, O.; Nakai, H.; Klene, M.; Li, X.; Knox, J. E.; Hratchian, H. P.; Cross, J. B.; Adamo, C.; Jaramillo, J.; Gomperts, R.; Stratmann, R. E.; Yazyev, O.; Austin, A. J.; Cammi, R.; Pomelli, C.; Ochterski, J. W.; Ayala, P. Y.; Morokuma, K.; Voth, G. A.; Salvador, P.; Dannenberg, J. J.; Zakrzewski, V. G.; Dapprich, S.; Daniels, A. D.; Strain, M. C.; Farkas, O.; Malick, D. K.; Rabuck, A. D.; Raghavachari, K.; Foresman, J. B.; Ortiz, J. V.; Cui, Q.; Baboul, A. G.; Clifford, S.; Cioslowski, J.; Stefanov, B. B.; Liu, G.; Liashenko, A.; Piskorz, P.; Komaromi, I.; Martin, R. L.; Fox, D. J.; Keith, T.; Al-Laham, M. A.; Peng, C. Y.; Nanayakkara, A.; Challacombe, M.; Gill, P. M. W.; Johnson, B.; Chen, W.; Wong, M. W.; Gonzalez, C.; Pople, J. A. *Gaussian 03*; Gaussian, Inc.: Pittsburgh, PA, 2003.
(6) Peng, C.; Schlegel, H. B. *Isr. J. Chem*. **1994**, *33*, 449.
(7) Peng, C.; Ayala, P. Y.; Schlegel, H. B.; Frisch, M. J. *J. Comput. Chem*. **1996**, *17*, 49.
(8) Bartolotti, L. J.; Edney, E. O. *Chem. Phys. Lett*. **1995**, *245*, 119.
(9) García-Cruz, I.; Castro, M.; Vivier-Bunge, A. *J. Comput. Chem*. **2000**, *21*, 716.
(10) Suh, I.; Zhang, R.; Molina, L. T.; Molina, M. J. *J. Am. Chem. Soc*. **2003**, *125*, 12655.
(11) Huang, M.; Zhang, W.; Yang, Y.; Wang, Z.; Hao, L.; Zhao, W.; Zhao, W.; Li, J.; Gao, X. *J. Mol. Struct.* **2006**, *774*, 1.